Molecular dynamics as an approach to study prion protein misfolding and the effect of pathogenic mutations

Marc W. van der Kamp and Valerie Daggett*

Department of Bioengineering, University of Washington, Box 355013, Seattle, WA 98195-5013

Abstract

Computer simulation of protein dynamics offers unique high-resolution information that complements experiment. Using experimentally derived structures of the natively folded prion protein, physically realistic dynamics and conformational changes can be simulated, including the initial steps of misfolding. By introducing mutations *in silico*, the effect of pathogenic mutations on prion protein conformation and dynamics can be assessed. Here, we briefly introduce molecular dynamics methods and review the application of molecular dynamics simulations to obtain insight into various aspects of the prion protein, including the mechanism of misfolding, the response to changes in the environment, and the influence of disease-related mutations.

1 Introduction

Transmissible spongiform encephalopathies (TSEs) are fatal neurodegenerative diseases that occur in mammalian species, including scrapie in sheep, bovine spongiform encephalopathy in cattle, chronic wasting disease in deer and elk and Creutzfeldt-Jakob disease (CJD) in humans. These prion diseases can arise spontaneously as a rare 'sporadic' disorder, caused by hereditary or somatic mutations, or through infectious transmission. The notion that the infectious disease agent in TSE could be devoid of nucleic

acids and primarily exists of protein, the so-called protein-only hypothesis, was first advanced in the 1960s based on experimental observations [1] and theory [2]. Prusiner and colleagues later showed that a particular protein was indeed required for infectivity [3-5]. Based on the name given to such a protein-based nucleic-acid free agent, a *pro*teinaceous *in*fectious particle or *prion*, the protein was called the prion protein (PrP). Further pathological studies showed that the typical, often fibrillar, amyloid deposits, found in the brains of inoculated individuals, contained host-encoded PrP [6]. Together, these findings sparked wide-ranging studies on PrP, both *in vivo* and *in vitro*.

The benign and natively folded cellular form, PrP^{C}, was isolated and characterized in detail. It is largely soluble and has high α-helical content with little β sheet [7-9] (see section 3.1). *In vivo*, it is primarily found attached to the outer cell membrane of neuronal cells [10], via a glycosylphosphatidyl-inositol (GPI) anchor linked to the protein C-terminus [11] (Fig. 1a). Determining the function of PrP^{C} has proved to be a major challenge, complicated by the fact that PrP knock-out mice lack an obvious phenotype [12]. Many different putative functions have been proposed, indicating that PrP^{C} is a multifunctional protein that plays a role in cell signaling [13, 14] and metal metabolism [15-17]. When PrP aggregates and forms fibrils, however, it has significantly changed conformation and becomes largely insoluble and proteinase K resistant. It is likely that early, non-fibrillar aggregates represent the infectious particles and cause neurotoxicity [18]. Together, the various aggregates consisting of misfolded PrP are often denoted PrP^{Sc}, for scrapie. Apart from the fact that PrP^{Sc} has a significantly increased β-sheet content and decreased α-helical content [7, 19, 20], little is known about its precise conformation from experiment. The conversion from PrP^{C} to PrP^{Sc} appears to be triggered by a decrease in pH [21, 22], introduction of mutations [23, 24] and by the presence of PrP^{Sc} [25].

Despite the continuing research into various aspects of the prion protein, many open questions remain. These include the precise function of PrP^{C}, the mechanism of PrP^{C} to PrP^{Sc} conversion, the nature of the infectious and neurotoxic particles and the mechanism of neurotoxicity. Current research efforts therefore cover many different aspects and employ a wide variety of experimental methods, from structural biology to *in vivo* studies. Computational studies can provide a complementary tool to help elucidate some of the outstanding questions. In the last decade, computer simulation of biomolecules, in particular proteins, has advanced significantly [26]. A method that has had a particularly large impact is molecular dynamics (MD) simulation. This technique allows for the detailed examination of the complex internal motions and conformational changes in proteins, which is often important for understanding their function [27-29]. Furthermore, MD

simulations provide uniquely detailed information necessary to understand protein folding [30, 31] and, crucially, disease-related protein misfolding [32, 33]. Accurate all-atom MD simulations have now been performed on a large scale across essentially all known protein folds, opening the way to obtain fundamental insights into protein dynamics and folding [34].

MD simulation was first used in PrP research to study the conformational preferences of a small fragment, indicating how a disease-related mutation may favor aggregation [35]. Soon after detailed structural information became available [8, 36-39], MD simulation was employed to study the folded domain of PrP [40-43]. These initial studies were limited, allowing for studying local dynamical effects only. Currently, advances in computer power and algorithms provide the means to perform multiple simulations of 10s to 100s of nanoseconds. Although this may still be short in terms of biological time scales, the more extensive simulations make detailed comparisons to experiment possible. Furthermore, longer simulations are able to capture significant conformational changes, such as those involved in misfolding.

In this chapter, we start with a brief outline of the theoretical aspects of MD simulations. Then, we review how these methods have been used to explore the dynamics and misfolding of the prion protein, and how this information was used to suggest models for early aggregates. Thereafter, we highlight applications of MD simulations that provide insight into the effects of mutations related to human prion disease. We then briefly describe other aspects of the prion protein that have been studied using molecular dynamics, such as the influence of post-translational modifications and small molecules. We close with an outlook of how MD studies can further increase our knowledge of the prion protein in the future.

2 Molecular dynamics simulation

Simulation of molecular dynamics of proteins at the atomic level is a well-established technique [29, 44, 45]. By explicitly representing all atoms and bonds in a macromolecule, it provides physically realistic information on how this molecule, e.g. a protein, evolves over time. The resulting ‘trajectory’ is recorded at high temporal resolution and can be analyzed using a wide range of techniques, offering a uniquely detailed insight into local dynamics, stability, flexibility, and possible conformational changes in proteins.

2.1 Principles

A typical protein contains 100s to 1000s of atoms and therefore has an even larger number of degrees of freedom. When the solvent around a protein is considered explicitly, the number of atoms and degrees of freedom increases even further. In order to model such a complex system efficiently, electrons are generally ignored and properties of the system are calculated based on the nuclear positions only. In combination with a potential energy function that describes electronic phenomena such as chemical bonding, spatial configurations of atoms and electrostatic interactions, this simplification allows the use of classical mechanics to describe the system. This type of modeling is generally described as *molecular mechanics* [46]. The potential energy function and the parameters for the different atoms and configurations of atoms used in this function are called a *force field*. Current force fields optimized for proteins are well established and describe protein dynamics with similar accuracy [47]. They use similar potential energy functions, in which, for example, bonds and angles are represented by harmonic terms, electrostatic interactions are described by atomic partial charges and the Coulomb equation, and Van der Waals forces are included through a simple Lennard-Jones function [48, 49].

The force field defines the energy of a particular atomic configuration. In order to describe the dynamics of a protein system, it is necessary to 1) get a starting configuration of the atoms in the system, 2) set this configuration in motion and 3) calculate a new configuration based on that motion. High-resolution starting configurations for many proteins can be obtained from the Protein Data Bank (PDB) [50], the depository of protein structures usually determined by X-ray crystallography or protein NMR techniques. Not every structure in this database will be of high enough quality for simulation. Also, in many cases, positions for missing atoms will need to be assigned, e.g. hydrogen atoms (not observed in X-ray crystallography) and atoms in parts of the structure that are too flexible to be determined in the experiment. Once a starting conformation is obtained, and (in the case of simulation with explicit solvent) solvent molecules are added in optimized positions, the system can be set in motion. In order to do so, velocities are assigned randomly, typically restrained by the Maxwell-Boltzmann distribution at a chosen temperature. Given these initial velocities and atomic masses, the forces on all atoms in the systems are now described by the derivative of the potential energy defined by the force field. These forces can in turn be used to calculate a new set of atomic positions and velocities. In order to obtain a physically accurate new atomic configuration, the time step (the amount of time between one configuration and the next) must typically be $\leq$2 fs (smaller than the fastest movement in the system, e.g. bond vibration). In principle, MD simulation is a deterministic

technique: given one set of atom positions and velocities, one series of configurations through time, or a trajectory, will be the result.

2.2 Scope, limitations and variations

Within the limitations of the accuracy of force fields, MD simulation predicts the motion of a molecular system through time. The simulation lengths that can be assessed have greatly increased by the developments in computer hardware and efficient algorithms. However, current simulations are typically still limited to 10s to 100s of nanoseconds, whereas many biological processes occur on much longer time scales. The combination of the high temporal and high spatial resolution obtained in MD simulations, however, is unattainable by experimental techniques. One could see an MD simulation as a 'computational experiment' that can reveal the motion of biomolecules in great detail. Just as in lab experiments, it is important to repeat the experiment (i.e. the simulation) to substantiate any conclusions drawn. Now computational resources allow one to do so, it is therefore good practice to perform several simulations of the same system, starting from different initial velocities.

Another way to view MD simulation is as a technique to probe the atomic positions and momenta that are available to a molecular system under certain conditions. In other words, MD is a statistical mechanics method that can be used to obtain a set of configurations distributed according to a certain statistical ensemble. The natural ensemble for MD simulation is the microcanonical ensemble, where the total energy E, volume V and amount of particles N (NVE) are constant. Modifications of the integration algorithm also allow for the sampling of other ensembles, such as the canonical ensemble (NVT) with constant temperature (T) instead of constant energy, or in the isothermal-isobaric ensemble (NPT) in which pressure is constant instead of volume. The structural configurations of a protein that are accessible within these conditions are governed by the free energy landscape. When standard all-atom explicit solvent MD simulation is used, physically realistic conformational transitions between such configurations are sampled. The nature of the free energy landscape, however, reduces the likelihood of sampling rare transitions (such as misfolding). Given the limitations in time-scale, the system is more likely to sample conformations within a set of closely related local minima, a 'valley' within the free energy landscape. There are several ways in which more comprehensive sampling of conformational space can be achieved, although this usually comes at the cost of representing a physically relevant trajectory or pathway. A simple way to increase sampling is to raise the temperature used in simula-

tion. This effectively increases the energy available to the system to overcome free energy barriers. Another technique using this principle is replica-exchange MD [51]: several non-interacting replicas of the simulation system are run at different temperatures, and the replicas are allowed to exchange with one another when similar conformations are sampled. Another technique that helps to avoid the multiple minima in the free energy landscape is *metadynamics*, aimed at avoiding minima that have already been sampled within a trajectory [52]. However, these two methods can't provide pathways for a process, or the mechanism of a conformational change. Instead they are used for sampling different states. In order to enhance the timescales accessible by MD simulation, the number of particles to consider can be reduced by the use of implicit solvent methods or a *coarse-grained* representation of the system, in which multiple atoms (e.g. in an amino acid side chain) are treated as one particle.

3 The dynamics and misfolding of the wild-type prion protein

MD simulations have been employed extensively to study the conformational dynamics of the wild-type prion protein for a range of species. A wide variety of force fields, setups and analyses has been used to this end. The majority of studies is performed on human, mouse or hamster PrP. In all but a few contributions [53-55], simulations include only the protein portion, i.e. the unglycosylated form without membrane anchoring. These simulations therefore present the recombinant PrP (recPrP) that is used for many *in vitro* studies, usually produced in *E. coli*. Often, only the structured part of recPrP is simulated. Although most initial MD studies could only capture local dynamics [40-43], some studies were able to shed light on the misfolding process over short time scales (~10 ns) [56, 57]. More recent studies reporting multiple simulations of 50 ns or more [58, 59], have provided a more comprehensive view of the conformational dynamics.

Apart from studying the native dynamics of recPrP in solution, MD simulation has also been used to sample possible early events in prion protein misfolding, either by simulating under conditions that are known to promote misfolding, such as low pH [56, 57, 59-61], or by using enhanced, non-physical sampling methods [62, 63]. As details of the misfolding pathway are unknown and difficult to probe by experiment, the results obtained can only suggest potential events and conformations along the pathway. Careful comparison with available experimental data, however, may validate the simulation results.

3.1 The starting point: PrP structures from experiment

High-resolution structural information is required as a starting point for atomistic MD simulations. For PrP, the first [8] and most abundant structural information has been obtained by nuclear magnetic resonance techniques (NMR), which has resulted in experimentally derived models of PrP of a wide variety of species [64-70]. For human and sheep PrP, structures determined by X-ray crystallography have also been reported, both with and without antibodies bound [71-75]. The overall structure of PrP that has emerged from these studies is largely identical for the different species and conditions. The mature protein (residues 23-230 in human PrP numbering, used throughout in this chapter) exhibits a highly flexible N-terminal domain, consisting of the first ~100 residues, and a folded or globular C-terminal domain, spanning residues 125-228. The final residues (229-230) also appear to be flexible.

The globular domain contains a short β-sheet, existing of two strands (S1 and S2 with res. 128-131 and 161-164, respectively), and three α-helices (HA, HB and HC) (Fig. 1b). The first α-helix, HA, is the shortest. It spans residues 144-156, with the last 3 residues forming a 3_{10} helix at neutral pH and a less regular structure at pH 4.5 [39, 76]. The second and third α-helices, HB (res. 172-194) and HC (res. 200-228), are connected by a disulfide bond: Cys179-Cys214. This disulfide bond is retained when PrP misfolds and aggregates [77, 78]. Around it, several hydrophobic residues are located that link HB and HC together and form a stable core of the protein [79]. The C-terminal end of HB (res. 187-194) is significantly less stable than the rest; NMR studies reveal that it can exist in a disordered conformation [39] and hydrogen-exchange protection of the backbone amides is low [39, 76, 79]. The many threonine residues in this sequence (HTVTTTTK, conserved in mammalian PrPs) cause this part of HB to have an inherently low helical propensity [80]. Notably, this part of HB appears to be stabilized to some degree by the presence of the flexible N-terminus, likely due to contacts [39]. At the top of HC, a so-called 'capping box' interaction [81] may help stabilize the helical structure [82]. For the C-terminal portion of HC, there are also indications that its conformation can be flexible. Residues 220-231 are considered partly disordered in mouse PrP [8] and human PrP with the R220K mutation [83]. NMR relaxation studies on hamster and mouse PrP further indicate fast picosecond time-scale motions of the backbone amides from res. 222 [84, 85].

The detailed structural information obtained from experiment for the globular domain of PrP^C provides a starting point to perform molecular dynamics simulations. One must realize, however, that uncertainties in the structure of PrP in aqueous solution still exist. Using protein NMR techniques, a set of conformational constraints is obtained that is subsequently

used to generate likely structural models that satisfy these constraints [86]. Although this method generally provides a good description of the overall fold, the positions of certain residues or side-chains may be less well-defined. X-ray crystallography has similar limitations, although high-resolution electron density maps offer more certainty. The crystallization process may, however, influence the protein conformation, e.g. through crystal packing, dimerization and domain swapping. The structure obtained may therefore not be fully representative for the conformation in solution.

3.2 The influence of pH on PrP dynamics and conformation

A range of experiments have indicated a relationship between a decrease in pH and misfolding and aggregation of PrP [87]. In human recPrP, significant conformational changes were observed between pH 6 and 4.4 [22], involving exposure of hydrophobic surface, thereby facilitating aggregation. Human PrP extracted from brain cells forms detergent-insoluble aggregates at pH 3.5 and 1.5 M guanidinium hydrochloride [88]. Initial changes are accompanied by a decrease in thermodynamic stability of recPrP relative to neutral pH, as evidenced by continuous-flow fluorescence [89] and NMR [76]. Further, studies of human recPrP under acidic and mildly denaturing conditions suggest the presence of intermediate states during misfolding and oligomerization: a native like α-helical conformation was observed at pH 4.1 and a conformation with β-sheet characteristics at pH 3.6 [90]. For mouse and hamster recPrP, similar changes were observed in response to a decrease in pH [91, 92]. In particular, loosening of the tertiary structure of hamster recPrP occurred below a pH of 4.7, with a minor shift to β structure at pH 4.0. This was accompanied by a decrease in binding of antibodies to epitopes in the flexible N-terminus [92], indicating that this flexible tail changes during misfolding. More recently, spontaneous aggregation and fibril formation of human recPrP was achieved under conditions of pH 4.0 and slow rotation, without addition of denaturants [21]. Altogether, it is evident that pH affects conformation and stability of PrP, and acidic pH can cause misfolding and aggregation. This is relevant for the occurrence of misfolding and aggregation *in vivo*, as it has been suggested that these processes may take place in endosomal compartments [93-96], which are mildly acidic [97].

In standard molecular mechanics methods, all atoms and bonds between atoms are explicitly defined, i.e. they are either present or not. In order to model the changes in pH, one must therefore alter the protonation states of ionizable amino acid side chains. For a decrease in pH, the relevant side chains are those of histidine, glutamate and aspartate. Their pK_a values in

solution are 6.08, 4.15 and 3.71, respectively [98]. The local protein environment can, however, change the pK_a of individual residues significantly. Langella et al. [99] calculated theoretical pK_a values of the relevant side-chains based on the coordinates deposited for human recPrP obtained by protein NMR at pH 4.5 and pH 7.0 [39, 76]. Although differences in the local conformation of residues between the various structures lead to a range of pK_a values, their results suggest that two of the four histidine residues in the globular domain (His140 and His177) will be protonated at very mildly acidic pH (pH < 6.5). The other two (His155 and His187), however, may only become fully protonated around pH 4.5. At this mildly acidic pH, solvent-exposed glutamate residues may also become protonated and a further decrease to strongly acidic pH (pH ≤ 3.0) will likely result in protonation of all glutamate and aspartate side chains. In line with these values, several MD studies have used differential protonation of side chains to compare the conformational dynamics of human PrP between neutral and strongly acidic pH [56, 57, 61], neutral and mildly acidic pH [99, 100], and all three pH environments [59, 101]. The neutral pH environment was represented by using singly protonated (neutral) histidine side chains and all other ionizable side chains charged, mildly acidic pH by all ionizable side chains charged, and strongly acidic pH by all ionizable side chains protonated. One study also simulated species with only part of the histidine side chains charged [99]. For hamster and bovine PrP, MD simulations have also been performed in a strongly acidic pH environment [56, 57], predominantly to capture the process of PrP misfolding (see further section 3.3).

All studies on the effect of pH on WT PrP published before 2007 reported single MD simulations, mostly of 10 ns. In 2007, DeMarco and Daggett reported 3 simulations of 15 ns of human PrP at both neutral and strongly acidic pH [61]. As in all previous studies, the overall fold was stable at neutral pH. Significant changes were observed for one simulation at strongly acidic pH, which was linked to misfolding of the protein (see further below). Recently, we performed the most extensive MD simulations of the effect of pH on human PrP to date, including detailed comparisons to experimental data [59]. In this study, 5 simulations of 50 ns at each of the three pH environments were compared. In the remainder of this section, we will focus on this study to highlight the information obtained by MD simulation on the effect of pH on the structure and dynamics of PrP.

At neutral pH, the overall fold is stable, without significant changes in secondary or tertiary structure. The flexibility of the S2-HB and HB-HC loops is high, in accordance with experimental data [84, 85]. Although the capping box at the N-terminal end of HC was not present in the starting structure (obtained from the representative NMR structure with PDB code 1QLX), it formed within 1 ns in all simulations at neutral pH. Also, a hy-

drogen bond between His187 and the main-chain carbonyl of Arg156, which anchors HA to HB, was present for ~30% of the simulation time. Comparisons with publicly available distance restraints obtained from NMR further indicated that relevant conformational ensembles were sampled and maintained throughout all 5 runs.

Theoretical pK_a calculations indicate that the first two histidine side chains to become protonated are His140 and His177. In a single 10 ns simulation, Langella et al. found little difference from a neutral pH simulation [99], as could be expected from their initial placement out into solvent. With all histidine side chains protonated, however, simulations revealed more significant changes [59]. In this mildly acidic pH environment, the 3_{10}-helix conformation in res. 153-156 that was formed for ~25% of the time at neutral pH, largely disappeared. This is in agreement with the NMR studies and the simulations indicate that this change is due to a repulsion between the side chains of His155 (now protonated) and Arg156. A more significant change, which was not directly apparent from the NMR structure obtained at pH 4.5, was observed in the loop between HB and HC. Phe198, central in this loop and part of the hydrophobic core at neutral pH, moved out into solvent. This change was accompanied by a change in the loop conformation and disruption of the capping box on top of HC. These changes may be related to the protonation of His187, the histidine with the lowest theoretical pK_a value (and therefore perhaps largely unprotonated in the NMR experiment). In the simulations at mildly acidic pH, a salt bridge interaction between His187 and Asp202, involved in the capping box at neutral pH, is formed.

The strongly acidic environment introduces significant changes in the PrP structure: protonation of the 5 Asp and 9 Glu side chains in the globular domain causes the overall atomic charge in this domain to rise by 14 a.u compared with the mildly acidic regime. A large effect on the conformation and dynamics can therefore be expected. Notably, changes to the most stable part of the PrP structure (as determined by NMR and hydrogen exchange [39, 76, 79, 85]) are minimal (Fig. 2). A major change observed in 3 of the 5 simulations, also found in several other studies [56, 57, 61, 102], is a repositioning of HA. The N-terminal part of helix swings away from the stable HB-HC core, out into solvent. Interestingly, this part was determined to be the most pH sensitive site in cysteine-scanning spin-labeling ESR studies [103]. Detailed analysis indicates that this movement is always preceded by a decrease in contacts between the hydrophobic residues in the S1-HA loop and those on HC (Fig. 2). Interestingly, unfolding studies also indicate that the S1-HA loop and HA can rearrange and become detached from the remainder of the protein [104, 105]. The changes in the S1-HA loop and HA may therefore be related to misfolding.

3.3 Misfolding and aggregation

Due to the importance of PrP misfolding for development of TSE diseases and the technical difficulties involved in probing this process experimentally, many MD studies have aimed at probing the initial events in conversion of PrP^{C} to PrP^{Sc}. Different strategies have been used to increase the likelihood of observing such initial misfolding when starting from the native PrP^{C} structure, which should be a rare event. One strategy is the introduction of single-residue mutations that have been shown to destabilize the native PrP^{C} fold and promote aggregation. For example, Hirschberger et al. studied the M205R and M205S mutations in the structured part of human PrP (res. 125-228) in single 10 ns MD simulations [106]. Cell studies had indicated that these mutations interfere with folding and can adopt a misfolded conformation [107]. In simulation, the native fold was indeed destabilized by both mutations, but in significantly different ways: with M205S unfolding of the central part of HB (res. 181-188) occurred whereas with M205R, HA moved out to solvent and subsequently lost helical structure. It is not clear if these events are related to the misfolding pathway of WT PrP, because the mutant proteins may never adopt the native fold. In section 4, we will discuss the use of MD to study the effects of single residue mutations further.

To increase conformational sampling, replica-exchange MD simulations were performed by De Simone et al. [63], based on the crystal structure of sheep PrP [73] (res. 125-230). One conformational substate found in the simulations was argued to be a possible intermediate for aggregation. It featured similar changes from the native fold as found in regular MD simulations of human PrP at acidic pH [59, 61]: HA was disconnected from the core of HB and HC and a large hydrophobic surface was exposed. The limitation of this work and other studies [62, 106], however, is that the flexible N-terminus was not included in the simulations. There are many indications from experiment that at least part of this region plays a role in misfolding and aggregation [108-111]. We have therefore always included part of the flexible N-terminus in our simulations. Further, the relation between acidic pH, a decrease in PrP^{C} stability and conversion of PrP^{C} to PrP^{Sc}, as outlined above, makes it plausible to use simulations in the strongly acidic environment as the conversion-inducing perturbation.

The first MD study to report on the initial, pH-induced conformational conversion of PrP^{C} [56] used a starting structure of res. 109-219 from recombinant Syrian hamster PrP determined by NMR [37]. Whereas simulation at neutral pH resulted in a stable 10 ns trajectory, a significant increase in flexibility and conformational changes were observed at strongly acidic pH. Importantly, the native β-sheet extended and additional strands were formed in the N-terminal region. Also, HA and the preceding S1-HA loop

became disconnected from the rest of the globular domain. Several residues in the S1-HA loop adopted a β-strand-like structure. Similar structural conversions were later also reported in equivalent simulations and fragments of bovine and human PrP [57] and for a longer fragment of human PrP (res. 90-231) [61]. Recently, it was shown that this type of initial structural conversion can also take place under mildly acidic simulation conditions (only His protonated) [59]. The similarities between simulations of a number of different fragments and different conditions provide credence to the early steps of misfolding observed.

Although the 3 helices remain largely intact in the simulations of early misfolding, the amount of β-structure increases. An additional β-strand is formed onto the native sheet, usually located in residues 116-122 of the flexible N-terminus. Further strands sometimes form in the remaining part that was included in the simulation. Antibody studies indicate that residues 90-120 undergo a conformational change upon conversion to PrP^{Sc} [112-114] and a range of studies support the involvement of residues in this region in PrP^{Sc} formation [108, 110, 111, 115]. Our misfolding simulations also indicate the formation of an isolated strand in the loop preceding HA (res. 136-140), after hydrophobic contacts with HC are lost. Abalos et al. [108] showed that modifications in this loop, such as sequence scrambling and mutations to alanine, interfered with conversion to PrP^{Sc}. Also, NMR studies indicate that the S1-HA loop changes under high-pressure conditions, including the loss of hydrophobic contacts [116]. These experimental data confirm that the pH- and aggregation-related exposure of hydrophobic surface [22] can arise from a conformational change in the S1-HA loop, as first suggested by MD simulation [56].

In addition to the MD studies mentioned above, simulation of the 109-219 fragment of hamster PrP was also performed with the D147N mutation [117]. This mutation does not significantly destabilize the PrP fold, but it does increase conversion efficiency [23]. 20 ns MD simulation at neutral and strongly acidic pH revealed structures that deviated significantly from the starting structure. At strongly acidic pH, a conformational state arose that was similar to those observed in pH-induced misfolding simulations of WT PrP [56, 57]. Again, the conformation exhibited a three-stranded sheet (formed by extension of the native sheet) and an isolated strand in residues 135-140 (the S1-HA loop). Using a typical structure from this conformational state as a monomer, an oligomeric structure was built by bringing together exposed hydrophobic residues. This included the docking of the isolated β-strand to the additional β-strand formed from the flexible N-terminus. Further addition of monomers led to a spiral oligomeric structure with a 3_1 symmetry axis and a β-sheet core (Fig. 3a). This 'protofibril' could be an early aggregate on the pathway to amyloid formation and/or relevant to infectious and neurotoxic particles. The model fits remarkably

well to the electron-microscopy data of two-dimensional PrP^{Sc} crystals [118], including the position of res. 142-176 and glycans inferred from electron-microscopy difference maps of PrP27-30 and $PrP^{Sc}106$ [117]. Subsequently, the compatibility between the protofibril model and a range of experimental data further indicated the relevance of this model [119], in contrast to a previously proposed fibril model based on a β-helix structure [120].

After our protofibril model was shown to be plausible, similar models were built for WT hamster, human and bovine PrP [121]. Again, the initial monomer structure was obtained from MD simulation at the strongly acidic pH regime. In contrast to hamster PrP, human and bovine PrP showed a left-handed spiral formation (Fig. 3b). This difference and further subtle differences between the individual protofibril models may reflect strain differences and give clues to the origin of observed "species barriers" [122]: transmission of prion disease between different species can be inefficient or even absent. Furthermore, the models may help to rationalize the perceived importance of the S2-HB loop conformation regarding cross-species infectivity [9, 65, 66, 69], as this loop forms a crucial contact area between multiple monomers in the protofibril models.

4 The effect of pathogenic mutations

About 10-15% of prion diseases in humans are caused by mutations in the *PRNP* gene (see further chapter X by Collinge et al.). Three different types of pathogenic mutations exist: premature stop codons, insertion of additional octapeptide repeats in the flexible N-terminus, and point-mutations leading to single amino acid replacements. The latter type of pathogenic mutation has been found in at least 28 different locations, and effects on protein stability, misfolding as well as cellular processing and function are reported [123]. MD simulations can be used to study the effect of these mutations on protein conformation and stability, particularly for the 24 mutations that are found in the C-terminal folded domain of human PrP [124-126]. Structural biology can also offer insights into the structural effect of pathogenic mutations [75, 127] (see also chapter Y by Surewicz et al.). In some cases, however, structural studies do not reveal differences between wild-type and mutant proteins whereas MD simulations do (see e.g. [128-130]).

4.1 D178N

The D178N mutation in human PrP is involved in familial prion disease [131]. Intriguingly, the phenotype of disease is significantly altered by the common M/V polymorphism at res. 129: fatal familial insomnia (FFI) arises in combination with M129 and familial CJD arises in combination with V129 [132], although this distinction may not be so clear cut [133, 134]. The aggregation propensity of PrP is significantly increased by the D178 to N substitution. When producing mutant human recPrP (res. 90-231) in *E. coli*, the D178N/M129 mutant aggregated into inclusion bodies [135], as was the case for D178N/M129 and D178N/V129 mouse recPrP [136]. Urea-induced unfolding studies indicated that the thermodynamic stability of PrP decreases by ~22 kJ mol^{-1} upon introduction of the mutation [136]. It was further found that the structure of D178N PrP^{Sc} is different from WT PrP^{Sc} obtained under the same conditions [137, 138].

The D178 side chain can form a salt bridge with R164 (located on the second native β-strand, S2) and may be involved in hydrogen bond interactions with the Y128 and Y169 side chains (located at the beginning of β-strand S1 and the loop between S2 and HB respectively) [56]. The interactions with both strands of the native β-sheet may be disrupted by the D178N mutation, thereby potentially affecting its stability. Spin-labeling ESR studies of D178N PrP indeed showed that the D178N mutation increases instability in S2 [139]. Crystal structures of D178N PrP with either M129 or V129 show little difference with the overall static fold of WT PrP [75]. Differential packing of the monomers, however, indicates that the native β-sheet may combine to form an intermolecular 4-stranded sheet with M129, but not with V129.

The experimental findings indicating that the D178N mutation affects PrP^{C} stability and promotes aggregation have prompted several MD studies studying the effect of the mutation on the PrP structure. To study the local structural effects, Billeter and Wüthrich performed short (0.5 ns) simulations of D178N,E200K mouse PrP combined with either M129 or V129 [140], in a small sphere of water. As expected, interactions with Y128 and R164 were disrupted (in contrast to the equivalent WT PrP simulations), but no further instability was found. Subsequent 1.5 ns explicit solvent MD simulations of WT mouse PrP (3 trajectories) and D178N mouse PrP (2 trajectories) also showed no differences in flexibility or conformation [141]. Interestingly, the R164-D178 salt bridge was only populated for 15% of the time in the most stable WT simulation in this study. The authors concluded that the R164-D178 salt bridge may not be important for WT PrP stability, but these simulations seem too short to substantiate such a statement.

Several MD studies were also run under conditions intended to perturb the starting structure further (in addition to the mutation). In high temperature, implicit solvent MD simulations of mouse PrP, HA was stable in WT but not in D178N PrP [142]. The authors attributed this to changes in the charge distribution that affect internal salt bridges in HA. In explicit solvent high temperature MD simulations of human D178N PrP (in combination with M129 or V129), however, no significant differences were observed [143]. In order to reveal weaknesses in the conformation of the globular domain, Barducci et al. performed simulations of WT and D178N mouse PrP in a hydrophobic environment (a solution of CCl_4) [144]. Multiple simulations of 3-8.1 ns revealed little difference in the overall conformation for WT PrP. With the D178N mutation, however, the S1/S2 β-sheet became unstable, presumably due to the lack of interactions with R164 and Y128. The weakening of the β-sheet in relation to disruption of the D178-R164 and D178-Y128 interactions was later confirmed using the metadynamics simulation technique [62].

4.2 Mutations in the hydrophobic core

The 3-dimensional structures of PrP of a variety of species have indicated that a conserved core of hydrophobic residues may confer stability to the globular domain [145]. This hydrophobic core consists of comprehensive interactions between HB and HC, interactions between HC and the loop preceding HA as well as contacts the native sheet and the rest of the globular domain (Fig. 1b). Four mutations in residues that are part of the hydrophobic core have been related to familial prion diseases in humans: V180I, F198S, V203I and V210I [123, 146-149]. Further, Thr183 forms additional interactions with the hydrophobic core, and its mutation to Ala causes familial CJD [150]. Experiments on mouse PrP mutants indicate that thermodynamic stability of PrP is significantly reduced for T183A and F198S and somewhat reduced for V180I [136]. For V180I, V210 and F198S PrP, it was found that a folding intermediate increased in the population relative to the native fold, further indicating that these mutations cause instability [89, 151]. Studies of V203I PrP are limited, but may suggest an effect on stability as well [152]. For T183A, the observed instability may be related to the loss of the hydrogen bond between Thr183 (in HB) and Y162 (in S2). The replacement of a hydrophobic residue with a hydrophilic residue in F198S PrP leaves a ‘gap’ in the hydrophobic core between HB and HC. The other three mutations are more conservative (Val to Ile), and it is therefore more difficult to interpret their potential effects from the WT structure alone.

To investigate the influence of the disease-related mutations in the hydrophobic core on the conformation and dynamics of recPrP, Van der Kamp and Daggett recently performed extensive MD simulations [126]. In a comparison of three 50 ns runs for each mutant with equivalent simulations of WT human PrP (res. 90-230), all mutations were observed to have some effect on structure and stability. In line with the effect on the thermodynamic stability of PrP, T183A and F198S significantly increased the flexibility of the globular domain, including the parts of HB and HC that are particularly stable in WT PrP (Fig. 4a). For F198S, flexibility was most strongly affected in the loop between HB and HC and the adjacent parts of the helices, as could expected based on the structural role of the Phe198 side chain [145]. Interestingly, a further significant effect was a shift of the native β-sheet (~20 Å from the mutation site) away from the rest of the globular fold. Such as shift was also observed for T183A and, to a lesser extent, for V180I, and could be related to a loss of the hydrogen bond between Thr183 and Tyr162. The addition of an extra CH_3 group in the Val to Ile mutations can cause steric crowding in the hydrophobic core. For V180I and V210I, this appears to cause a change in the hydrophobic packing of residues between HB and HC, which in turn causes Phe198 to move out of the hydrophobic core during the simulations. Further knock-on effects also cause a reduction of the hydrophobic contacts between the S1-HA loop and HC. In turn, this change can lead to HA moving out into solvent, similarly as observed in acidic conditions [59]. V203I was also observed to cause these effects, albeit to a lesser extent.

In one of the V180I simulations, a change in positioning of HA and the S1-HA loop is preceded by the addition of an extra strand onto the native sheet (Fig. 4b). This results in a similar early misfolded state as observed in simulation at acidic pH. In this conformation, significant parts of the original hydrophobic core are exposed to solvent, which will contribute to its aggregation propensity. Similar conformations related to early misfolding were also found in simulations of V210I. At the same time, the core of HB and HC in the V210I simulations showed similar stability and conformation as in the WT PrP simulations at three pH ranges [59]. These similarities between conformation and early misfolding are in line with the findings that PrP^{Sc} in patients carrying the V210I mutation consist of both V210I and WT PrP [153]. In contrast, the significant instability and conformational changes observed for T183A and F198S, also observed in coarse-grained MD simulation of T183A [154], may indicate a different disease mechanism. Cell studies indicate that the instability of the globular fold interferes with GPI-anchor attachment and subsequent cellular processing [155, 156]. *In vivo*, these mutations typically cause a prolonged duration of disease [157] and can lead to abnormal PrP^{Sc} formation [158]. Although correlations between simulation of recPrP and disease are specu-

lative, they indicate how MD simulation helps to uncover detailed molecular effects that may be important for the development of familial prion disease.

5 Other applications

5.1 In vivo *modifications*

Although most MD simulation studies and many experimental studies have focused on the recombinant PrP, the protein can undergo important post-translational modifications *in vivo*. After translation and transport to the endoplasmic reticulum, N-glycosylation may occur on two different sites in the globular domain (Asn181 on HB and Asn197 in the HB-HC loop), yielding un-, mono- and diglycosylated forms of PrP [159]. Modification of the initially attached high-mannose glycans occurs in the Golgi and creates a very diverse set (>400) of PrP glycoforms [160]. The effect of glycosylation on the structure of PrP was first studied by MD simulation [55]. Short (1.8 ns) simulations of an homology model of human recPrP (res. 90-230) with or without typical complex glycoforms indicated that glycosylation did not perturb the structure, and may even stabilize it somewhat. Although these simulations were too short to capture potential large conformational changes, NMR studies on bovine PrP purified from brain extracts indicated that the structure of glycosylated PrP (including the sugar portion of the GPI-anchor) is very similar to recPrP [161]. Recently, longer extensive MD simulations of diglycosylated PrP were reported [53]: DeMarco and Daggett performed 15 ns simulations of human PrP (res. 90-230) with complex glycans at neutral and low pH and concluded that the conformation and dynamics of PrP were not affected. It is possible, however, that contacts between the glycan attached to Asn197 and HA perturb pH-induced misfolding, which may affect binding efficiency to PrP^{Sc} and the morphology of the fibrillar aggregate [53]. Furthermore, the authors also reported equivalent simulations of diglycosylated PrP attached to a membrane via the GPI-anchor. This revealed that protein-membrane interactions probably only occur with the flexible N-terminus.

Another possible post-translational modification is the oxidation of methionine side chains, which can occur *in vivo* due to the presence of various reactive oxygen species. It is a reversible process due to the action of methionine sulfoxide reductases, but the methionine sulfoxide content of pro-

teins increases with age [162]. In contrast to PrP^{C}, a large fraction of methionine side chains were found to be oxidized in PrP^{Sc}, especially at Met213 [163]. A more recent study, however, concluded that Met213 is found in its oxidized state equally in PrP^{C} and PrP^{Sc} [164]. It is therefore unclear if methionine oxidation can be involved in triggering misfolding or stabilizing prion aggregates or not. To investigate if methionine oxidation could destabilize the PrP^{C} fold, MD simulations were performed of human PrP (res. 125-228) without Met oxidation, with Met213 oxidized and with Met206 oxidized [58]. Both residues are buried in the hydrophobic core of the native PrP structure. The simulations (2 runs of 80 ns for each species) indicated that methionine oxidation did not have a significant effect on the local structure, but a shift to more flexible conformational states occurred. Seemingly, the effect was transmitted to more distant regions in the structure, such as the S2-HB and HB-HC loops. It was suggested that methionine oxidation could trigger misfolding. This hypothesis was later corroborated by experimental studies of recPrP that used norleucine and methoxinine as analogues of the hydrophobic, non-oxidized form or the hydrophilic oxidized form of methionine, respectively [165]. The norleucine variant exhibited a stabilized α-helical structure and low aggregation propensity, whereas the methoxinine variant largely consisted of β-structure and had a high tendency to aggregate. Recently, experiment and MD simulation were used to determine that the M206S and M213S mutations also destabilized the native PrP fold and enhanced aggregation propensity [166].

5.2 The effect of small molecule ligands

The interaction of PrP with small molecule ligands can be of great interest with respect to the development of possible drugs targeting prion diseases, for example by inhibiting misfolding. MD simulations can be used in order to explain and rationalize the effects of small molecules. One example of this is the effect of the 'chemical chaperone' trimethylamide *N*-oxide (TMAO) on PrP misfolding. Experimentally, it was found that addition of TMAO efficiently reduced PrP^{Sc} formation in mouse neuroblastoma cells (75% reduction with 120 mM TMAO) [167]. Simulations in the presence of 1M TMAO were performed with hamster recPrP (res. 109-219) [168], starting from either the native conformation or a previously determined pH-induced misfolded conformation [56]. Both simulations were carried out with protonation states of the amino acids corresponding to the strongly acidic pH regime, to perturb the PrP structure. TMAO itself was not protonated (whereas its pK_a is ~4.7), as this is likely to cause destabilization ra-

ther than stabilization of protein structure [169, 170]. Starting from the misfolded conformation, the extended sheet is disrupted and PrP regains contacts that had been lost during the pH-induced misfolding (Fig. 5). In the simulation starting from the native structure, no misfolding is observed. In both cases, the hydrophobic residues in the flexible N-terminus formed an Ω-loop, that prevents this region from forming additional β-strands. The simulations further confirmed that the stabilizing action of TMAO is likely to be indirect: interactions of water molecules with the peptide backbone become less favorable in the presence of TMAO [171, 172].

Whereas the osmolyte TMAO cannot be used *in vivo* due to the toxic effect of trimethylamine, other compounds that inhibit formation of PrP^{Sc} can be administered to mammals. An example is *N,N′*-(methylenedi-4,1-phenylene)bis[2-(1-pyrrolidinyl)acetamide], or GN8. This compound was found to inhibit PrP^{Sc} production in vitro and prion-infected mice treated with GN8 showed prolonged survival [173]. The molecule was selected based on virtual screening of compounds that would bind in the region of the HA-S2 loop and the HB-HC loop of mouse PrP. According to the virtual screening results, GN8 forms hydrogen bonds with Asn159 and Glu196, thereby cross-linking the two loop regions. Yamamoto and Kuwata [174] first performed a 100 ns MD simulation of the initially obtained binding mode in water, to refine the PrP-GN8 structure further. The obtained binding mode agreed with NMR chemical shift data [173]. Also, the flexibility of the PrP structure was decreased in comparison with the equivalent simulation without GN8. To examine the stabilizing effect of GN8 further, simulations were also performed of mouse PrP in 6 M urea, either with or without GN8 bound [174]. These simulations indicate that the presence of urea destabilizes all three helices, whereas binding of GN8 prevents this destabilization to some extent. GN8 also appears to act as a 'chemical chaperone' that reduces the flexibility of the native PrP structure and increases its stability.

6 Conclusions and outlook

When properly prepared and executed, molecular dynamics simulations are able to capture realistic information on the dynamics and conformational ensembles of prion proteins. The benefit of such simulations comes from the unique spatial and temporal resolution, providing significantly more detailed information than is available from experiment. Early MD simulations have already provided insight into local and global changes, including possible steps in the misfolding and aggregation of prion proteins. Advances in computer speed and algorithms have made it possible to

perform more and longer simulations in recent years. This has opened up the possibility for increased sampling of the conformational dynamics of prion proteins. These new, extensive MD simulations have contributed significantly to our knowledge on the detailed atomic-level molecular mechanisms that are involved in the response to decreases in pH, single residue mutations, in vivo modifications and small molecules.

The continuing increase in computer resources makes it possible to simulate bigger systems and longer timescales. This will allow, for example, for a more detailed characterization of the conformation and dynamics of PrP^{C} under near-physiological conditions: glycosylated and bound to a membrane. These studies are currently underway in our group. Further, direct simulation of the process which is at the very heart of prion infection, conversion of PrP^{C} on a template of PrP^{Sc}, is also now possible.

The detailed information, gained from MD simulations, on the early mechanism of misfolding and related instabilities can be exploited for the design of small molecules or peptides that may serve as novel diagnostic tools and drugs. Once such molecules are designed, MD simulations can be employed to test and explain their action in detail. Overall, we expect that MD simulation methods will continue to be a valuable tool to provide information on various different aspects of the prion protein: the behavior and conformation of cellular PrP, misfolding of PrP, influence of mutations and development of prion disease diagnostics and therapies.

References

1. Alper T, Cramp WA, Haig DA, Clarke MC (1967) Does agent of scrapie replicate without nucleic acid? Nature 214: 764
2. Griffith JS (1967) Self-replication and scrapie. Nature 215: 1043
3. Prusiner SB (1982) Novel proteinaceous infectious particles cause scrapie. Science 216: 136
4. Bolton DC, McKinley MP, Prusiner SB (1982) Identification of a protein that purifies with the scrapie prion. Science 218: 1309
5. Oesch B, Westaway D, Walchli M, McKinley MP, Kent SBH, Aebersold R, Barry RA, Tempst P, Teplow DB, Hood LE, Prusiner SB, Weissmann C (1985) A cellular gene encodes scrapie PrP 27-30 protein. Cell 40: 735
6. Prusiner SB, Scott M, Foster D, Pan KM, Groth D, Mirenda C, Torchia M, Yang SL, Serban D, Carlson GA, Hoppe PC, Westaway D, DeArmond SJ (1990) Transgenetic studies implicate interactions between homologous PrP isoforms in scrapie prion replication. Cell 63: 673
7. Caughey BW, Dong A, Bhat KS, Ernst D, Hayes SF, Caughey WS (1991) Secondary structure-analysis of the scrapie-associated protein PrP 27-30 in water by infrared-spectroscopy. Biochemistry 30: 7672
8. Riek R, Hornemann S, Wider G, Billeter M, Glockshuber R, Wüthrich K (1996) NMR structure of the mouse prion protein domain PrP(121-231). Nature 382: 180

9. Wüthrich K, Riek R (2001) Advances in Protein Chemistry, Vol 57 (Advances in Protein Chemistry), vol 57 p 55
10. Taylor DR, Hooper NM (2006) The prion protein and lipid rafts (Review). Mol Membr Biol 23: 89
11. Stahl N, Borchelt DR, Hsiao K, Prusiner SB (1987) Scrapie prion protein contains a phosphatidylinositol glycolipid. Cell 51: 229
12. Steele AD, Lindquist S, Aguzzi A (2007) The prion protein knockout mouse: A phenotype under challenge. Prion 1: 83
13. Linden R, Martins VR, Prado MAM, Cammarota M, Izquierdo I, Brentani RR (2008) Physiology of the prion protein. Physiol Rev 88: 673
14. Le Pichon CE, Firestein S (2008) Expression and localization of the prion protein PrPc in the olfactory system of the mouse. J Comp Neurol 508: 487
15. Millhauser GL (2007) Copper and the prion protein: Methods, structures, function, and disease. Annu Rev Phys Chem 58: 299
16. Viles JH, Klewpatinond M, Nadal RC (2008) Copper and the structural biology of the prion protein. Biochem Soc Trans 36: 1288
17. Singh A, Mohan ML, Isaac AO, Luo X, Petrak J, Vyoral D, Singh N (2009) Prion protein modulates cellular iron uptake: a novel function with implications for prion disease pathogenesis. PLoS ONE 4: e4468
18. Caughey B, Baron GS, Chesebro B, Jeffrey M (2009) Getting a grip on prions: Oligomers, amyloids, and pathological membrane interactions. Annu Rev Biochem 78: 177
19. Jackson GS, Hill SF, Joseph C, Hosszu L, Power A, Waltho JP, Clarke AR, Collinge J (1999) Multiple folding pathways for heterologously expressed human prion protein. Biochimica Et Biophysica Acta: Protein Structure and Molecular Enzymology 1431: 1
20. Pan KM, Baldwin M, Nguyen J, Gasset M, Serban A, Groth D, Mehlhorn I, Huang ZW, Fletterick RJ, Cohen FE, Prusiner SB (1993) Conversion of alpha-helices into beta-sheets features in the formation of the scrapie prion proteins. Proc Natl Acad Sci USA 90: 10962
21. Cobb NJ, Apetri AC, Surewicz WK (2008) Prion protein amyloid formation under native-like conditions involves refolding of the C-terminal alpha-helical domain. J Biol Chem 283: 34704
22. Swietnicki W, Petersen R, Gambetti P, Surewicz WK (1997) pH-dependent stability and conformation of the recombinant human prion protein PrP(90-231). J Biol Chem 272: 27517
23. Speare JO, Rush TS, Bloom ME, Caughey B (2003) The role of helix 1 aspartates and salt bridges in the stability and conversion of prion protein. J Biol Chem 278: 12522
24. Vanik DL, Surewicz WK (2002) Disease-associated F198S mutation increases the propensity of the recombinant prion protein for conformational conversion to scrapie-like form. J Biol Chem 277: 49065
25. Saborio GP, Permanne B, Soto C (2001) Sensitive detection of pathological prion protein by cyclic amplification of protein misfolding. Nature 411: 810
26. Van der Kamp MW, Shaw KE, Woods CJ, Mulholland AJ (2008) Biomolecular simulation and modelling: status, progress and prospects. J R Soc Interface 5: S173
27. Glazer DS, Radmer RJ, Altman RB (2009) Improving structure-based function prediction using molecular dynamics. Structure 17: 919
28. Karplus M, Kuriyan J (2005) Molecular dynamics and protein function. Proc Natl Acad Sci U S A 102: 6679
29. Karplus M, McCammon JA (2002) Molecular dynamics simulations of biomolecules. Nat Struct Biol 9: 646

30. Daggett V, Fersht A (2003) The present view of the mechanism of protein folding. Nature Reviews Molecular Cell Biology 4: 497
31. Schaeffer RD, Fersht A, Daggett V (2008) Combining experiment and simulation in protein folding: closing the gap for small model systems. Curr Opin Struct Biol 18: 4
32. Chiti F, Dobson CM (2006) Protein misfolding, functional amyloid, and human disease. Annu Rev Biochem 75: 333
33. Daggett V (2006) Protein folding-simulation. Chem Rev 106: 1898
34. Van der Kamp MW, Schaeffer RD, Jonsson AL, Scouras AD, Simms AM, Toofanny RD, Benson NC, Anderson PC, Merkley ED, Rysavy S, Bromley D, Beck DAC, Daggett V (2010) Dynameomics: A comprehensive database of protein dynamics. Structure 18: 423
35. Kazmirski SL, Alonso DOV, Cohen FE, Prusiner SB, Daggett V (1995) Theoretical-studies of sequence effects on the conformational properties of a fragment of the prion protein: Implication for scrapie formation. Chem Biol 2: 305
36. Donne DG, Viles JH, Groth D, Mehlhorn I, James TL, Cohen FE, Prusiner SB, Wright PE, Dyson HJ (1997) Structure of the recombinant full-length hamster prion protein PrP(29-231): The N terminus is highly flexible. Proc Natl Acad Sci USA 94: 13452
37. James TL, Liu H, Ulyanov NB, FarrJones S, Zhang H, Donne DG, Kaneko K, Groth D, Mehlhorn I, Prusiner SB, Cohen FE (1997) Solution structure of a 142-residue recombinant prion protein corresponding to the infectious fragment of the scrapie isoform. Proc Natl Acad Sci USA 94: 10086
38. Riek R, Hornemann S, Wider G, Glockshuber R, Wüthrich K (1997) NMR characterization of the full-length recombinant murine prion protein, mPrP(23-231). FEBS Lett 413: 282
39. Zahn R, Liu AZ, Luhrs T, Riek R, von Schroetter C, Garcia FL, Billeter M, Calzolai L, Wider G, Wüthrich K (2000) NMR solution structure of the human prion protein. Proc Natl Acad Sci USA 97: 145
40. El-Bastawissy E, Knaggs MH, Gilbert IH (2001) Molecular dynamics simulations of wild-type and point mutation human prion protein at normal and elevated temperature. J Mol Graph Model 20: 145
41. Guilbert C, Ricard F, Smith JC (2000) Dynamic simulation of the mouse prion protein. Biopolymers 54: 406
42. Parchment OG, Essex JW (2000) Molecular dynamics of mouse and syrian hamster PrP: Implications for activity. Proteins: Struct Funct Genet 38: 327
43. Zuegg J, Gready JE (1999) Molecular dynamics simulations of human prion protein: Importance of correct treatment of electrostatic interactions. Biochemistry 38: 13862
44. Beck DAC, Daggett V (2004) Methods for molecular dynamics simulations of protein folding/unfolding in solution. Methods 34: 112
45. Rapaport DC (2004) The art of molecular dynamics simulation. Cambridge University Press, Cambridge, UK
46. Leach AR (2001) Molecular Modelling: Principles and Applications. Prentice Hall, Upper Saddle River, NJ
47. MacKerell AD (2005) In: Simmerling C (ed) Annual reports in computational chemistry, vol 1. Elsevier, Oxford, UK p 91
48. Mackerell AD (2004) Empirical force fields for biological macromolecules: Overview and issues. Journal of Computational Chemistry 25: 1584
49. Levitt M, Hirshberg M, Sharon R, Daggett V (1995) Potential-energy function and parameters for simulations of the molecular-dynamics of proteins and nucleic-acids in solution. Computer Physics Communications 91: 215

50. Berman HM, Westbrook J, Feng Z, Gilliland G, Bhat TN, Weissig H, Shindyalov IN, Bourne PE (2000) The protein data bank. Nucleic Acids Res 28: 235
51. Sugita Y, Okamoto Y (1999) Replica-exchange molecular dynamics method for protein folding. Chemical Physics Letters 314: 141
52. Laio A, Parrinello M (2002) Escaping free-energy minima. Proc Natl Acad Sci USA 99: 12562
53. DeMarco ML, Daggett V (2009) Characterization of cell-surface prion protein relative to its recombinant analogue: insights from molecular dynamics simulations of diglycosylated, membrane-bound human prion protein. J Neurochem 109: 60
54. Zhong LH, Xie JM (2009) Investigation of the effect of glycosylation on human prion protein by molecular dynamics. J Biomol Struct Dyn 26: 525
55. Zuegg J, Gready JE (2000) Molecular dynamics simulation of human prion protein including both N-linked oligosaccharides and the GPI anchor. Glycobiology 10: 959
56. Alonso DOV, DeArmond SJ, Cohen FE, Daggett V (2001) Mapping the early steps in the pH-induced conformational conversion of the prion protein. Proc Natl Acad Sci USA 98: 2985
57. Alonso DOV, An C, Daggett V (2002) Simulations of biomolecules: Characterization of the early steps in the pH-induced conformational conversion of the hamster, bovine and human forms of the prion protein. Philos Trans R Soc Lond A Math Phys Eng Sci 360: 1165
58. Colombo G, Meli M, Morra G, Gabizon R, Gasset M (2009) Methionine sulfoxides on prion protein helix-3 switch on the alpha-fold destabilization required for conversion. PLoS ONE 4: e4296
59. Van der Kamp MW, Daggett V (2010) The influence of pH on the human prion protein: Insights into the early steps of misfolding. Biophys J 99: 2289
60. Campos SRR, Machuqueiro M, Baptista AM (2010) Constant-pH molecular dynamics simulations reveal a β-rich form of the human prion protein. Journal of Physical Chemistry B DOI: 10.1021/jp104753t
61. DeMarco ML, Daggett V (2007) Molecular mechanism for low pH triggered misfolding of the human prion protein. Biochemistry 46: 3045
62. Barducci A, Chelli R, Procacci P, Schettino V, Gervasio FL, Parrinello M (2006) Metadynamics simulation of prion protein: beta-structure stability and the early stages of misfolding. J Am Chem Soc 128: 2705
63. De Simone A, Zagari A, Derreumaux P (2007) Structural and hydration properties of the partially unfolded states of the prion protein. Biophys J 93: 1284
64. Calzolai L, Lysek DA, Perez DR, Guntert P, Wuthrich K (2005) Prion protein NMR structures of chickens, turtles, and frogs. Proc Natl Acad Sci USA 102: 651
65. Christen B, Hornemann S, Damberger FF, Wuthrich K (2009) Prion protein NMR structure from Tammar wallaby (*Macropus eugenii*) shows that the beta 2-alpha 2 loop is modulated by long-range sequence effects. J Mol Biol 389: 833
66. Gossert AD, Bonjour S, Lysek DA, Fiorito F, Wuthrich K (2005) Prion protein NMR structures of elk and of mouse/elk hybrids. Proc Natl Acad Sci USA 102: 646
67. Lysek DA, Schorn C, Nivon LG, Esteve-Moya V, Christen B, Calzolai L, von Schroetter C, Fiorito F, Herrmann T, Guntert P, Wuthrich K (2005) Prion protein NMR structures of cats, dogs, pigs, and sheep. Proc Natl Acad Sci USA 102: 640
68. Wuthrich K, Riek R (2001) Advances in Protein Chemistry, Vol 57 (Advances in Protein Chemistry), vol 57 p 55
69. Christen B, Perez DR, Hornemann S, Wuthrich K (2009) NMR structure of the bank vole prion protein at 20 degrees C contains a structured loop of residues 165-171. J Mol Biol 383: 306

70. Perez DR, Damberger FF, Wuthrich K (2010) Horse prion protein NMR structure and comparisons with related variants of the mouse prion protein. J Mol Biol 400: 121
71. Antonyuk SV, Trevitt CR, Strange RW, Jackson GS, Sangar D, Batchelor M, Cooper S, Fraser C, Jones S, Georgiou T, Khalili-Shirazi A, Clarke AR, Hasnain SS, Collinge J (2009) Crystal structure of human prion protein bound to a therapeutic antibody. Proc Natl Acad Sci USA 106: 2554
72. Eghiaian F, Grosclaude J, Lesceu S, Debey P, Doublet B, Treguer E, Rezaei H, Knossow M (2004) Insight into the PrP^{C} -> PrP^{Sc} conversion from the structures of antibody-bound ovine prion scrapie-susceptibility variants. Proc Natl Acad Sci USA 101: 10254
73. Haire LF, Whyte SM, Vasisht N, Gill AC, Verma C, Dodson EJ, Dodson GG, Bayley PM (2004) The crystal structure of the globular domain of sheep prion protein. J Mol Biol 336: 1175
74. Knaus KJ, Morillas M, Swietnicki W, Malone M, Surewicz WK, Yee VC (2001) Crystal structure of the human prion protein reveals a mechanism for oligomerization. Nat Struct Biol 8: 770
75. Lee S, Antony L, Hartmann R, Knaus KJ, Surewicz K, Surewicz WK, Yee VC (2010) Conformational diversity in prion protein variants influences intermolecular beta-sheet formation. EMBO J 29: 251
76. Calzolai L, Zahn R (2003) Influence of pH on NMR structure and stability of the human prion protein globular domain. J Biol Chem 278: 35592
77. Herrmann LM, Caughey B (1998) The importance of the disulfide bond in prion protein conversion. Neuroreport 9: 2457
78. Welker E, Raymond LD, Scheraga HA, Caughey B (2002) Intramolecular versus intermolecular disulfide bonds in prion proteins. J Biol Chem 277: 33477
79. Hosszu LLP, Baxter NJ, Jackson GS, Power A, Clarke AR, Waltho JP, Craven CJ, Collinge J (1999) Structural mobility of the human prion protein probed by backbone hydrogen exchange. Nat Struct Biol 6: 740
80. Tizzano B, Palladino P, De Capua A, Marasco D, Rossi F, Benedetti E, Pedone C, Ragone R, Ruvo M (2005) The human prion protein alpha 2 helix: A thermodynamic study of its conformational preferences. Proteins: Struct Funct Bioinform 59: 72
81. Harper ET, Rose GD (1993) Helix stop signals in proteins and peptides: The capping box. Biochemistry 32: 7605
82. Gallo M, Paludi D, Cicero DO, Chiovitti K, Millo E, Salis A, Damonte G, Corsaro A, Thellung S, Schettini G, Melino S, Florio T, Paci M, Aceto A (2005) Identification of a conserved N-capping box important for the structural autonomy of the prion alpha 3-helix: The disease associated D202N mutation destabilizes the helical conformation. Int J Immunopathol Pharmacol 18: 95
83. Calzolai L, Lysek DA, Guntert P, von Schroetter C, Riek R, Zahn R, Wüthrich K (2000) NMR structures of three single-residue variants of the human prion protein. Proc Natl Acad Sci USA 97: 8340
84. O'Sullivan DBD, Jones CE, Abdelraheim SR, Brazier MW, Toms H, Brown DR, Viles JH (2009) Dynamics of a truncated prion protein, PrP(113-231), from N-15 NMR relaxation: Order parameters calculated and slow conformational fluctuations localized to a distinct region. Protein Sci 18: 410
85. Viles JH, Donne D, Kroon G, Prusiner SB, Cohen FE, Dyson HJ, Wright PE (2001) Local structural plasticity of the prion protein. Analysis of NMR relaxation dynamics. Biochemistry 40: 2743
86. Rule GS, Hitchens TK (2005) Fundamentals of Protein NMR Spectroscopy (Focus on Structural Biology). Springer, Dordrecht, The Netherlands

87. DeMarco ML, Daggett V (2005) Local environmental effects on the structure of the prion protein. Comptes Rendus Biologies 328: 847
88. Zou WQ, Cashman NR (2002) Acidic pH and detergents enhance in vitro conversion of human brain PrP^{C} to a PrP^{Sc}-like form. J Biol Chem 277: 43942
89. Apetri AC, Maki K, Roder H, Surewicz WK (2006) Early intermediate in human prion protein folding as evidenced by ultrarapid mixing experiments. J Am Chem Soc 128: 11673
90. Gerber R, Tahiri-Alaoui A, Hore PJ, James W (2008) Conformational pH dependence of intermediate states during oligomerization of the human prion protein. Protein Sci 17: 537
91. Hornemann S, Glockshuber R (1998) A scrapie-like unfolding intermediate of the prion protein domain PrP(121-231) induced by acidic pH. Proc Natl Acad Sci USA 95: 6010
92. Matsunaga Y, Peretz D, Williamson A, Burton D, Mehlhorn I, Groth D, Cohen FE, Prusiner SB, Baldwin MA (2001) Cryptic epitopes in N-terminally truncated prion protein are exposed in the full-length molecule: Dependence of conformation on pH. Proteins: Struct Funct Bioinform 44: 110
93. Arnold JE, Tipler C, Laszlo L, Hope J, Landon M, Mayer RJ (1995) The abnormal isoform of the prion protein accumulates in late-endosome-like organelles in scrapie-infected mouse-brain. J Pathol 176: 403
94. Borchelt DR, Taraboulos A, Prusiner SB (1992) Evidence for synthesis of scrapie prion proteins in the endocytic pathway. J Biol Chem 267: 16188
95. Caughey B, Raymond GJ, Ernst D, Race RE (1991) N-terminal truncation of the scrapie-associated form of PrP by lysosomal protease(s): Implications regarding the site of conversion of PrP to the protease-resistant state. J Virol 65: 6597
96. Godsave SF, Wille H, Kujala P, Latawiec D, DeArmond SJ, Serban A, Prusiner SB, Peters PJ (2008) Cryo-immunogold electron microscopy for prions: Toward identification of a conversion site. J Neurosci 28: 12489
97. Lee RJ, Wang S, Low PS (1996) Measurement of endosome pH following folate receptor-mediated endocytosis. Biochim Biophys Acta 1312: 237
98. Lide DR (2010). CRC Press, Taylor and Francis Group
99. Langella E, Improta R, Crescenzi O, Barone V (2006) Assessing the acid-base and conformational properties of histidine residues in human prion protein (125-228) by means of pK_a calculations and molecular dynamics simulations. Proteins: Struct Funct Bioinform 64: 167
100. Langella E, Improta R, Barone V (2004) Checking the pH-induced conformational transition of prion protein by molecular dynamics simulations: Effect of protonation of histidine residues. Biophys J 87: 3623
101. Gu W, Wang TT, Zhu J, Shi YY, Liu HY (2003) Molecular dynamics simulation of the unfolding of the human prion protein domain under low pH and high temperature conditions. Biophys Chem 104: 79
102. Colacino S, Tiana G, Broglia RA, Colombo G (2006) The determinants of stability in the human prion protein: Insights into folding and misfolding from the analysis of the change in the stabilization energy distribution in different conditions. Proteins: Struct Funct Bioinform 62: 698
103. Watanabe Y, Inanami O, Horiuchi M, Hiraoka W, Shimoyama Y, Inagaki F, Kuwabara M (2006) Identification of pH-sensitive regions in the mouse prion by the cysteine-scanning spin-labeling ESR technique. Biochem Biophys Res Commun 350: 549
104. Hosszu LLP, Wells MA, Jackson GS, Jones S, Batchelor M, Clarke AR, Craven CJ, Waltho JP, Collinge J (2005) Definable equilibrium states in the folding of human prion protein. Biochemistry 44: 16649

105. Torrent J, Alvarez-Martinez MT, Liautard JP, Balny C, Lange R (2005) The role of the 132-160 region in prion protein conformational transitions. Protein Sci 14: 956
106. Hirschberger T, Stork M, Schropp B, Winklhofer KF, Tatzelt J, Tavan P (2006) Structural instability of the prion protein upon M205S/R mutations revealed by molecular dynamics simulations. Biophys J 90: 3908
107. Winklhofer KF, Heske J, Heller U, Reintjes A, Muranyi W, Moarefi I, Tatzelt J (2003) Determinants of the in vivo folding of the prion protein - A bipartite function of helix 1 in folding and aggregation. J Biol Chem 278: 14961
108. Abalos GC, Cruite JT, Bellon A, Hemmers S, Akagi J, Mastrianni JA, Williamson RA, Solforosi L (2008) Identifying key components of the PrP^{C}-PrP^{Sc} replicative interface. J Biol Chem 283: 34021
109. Brown DR, Herms J, Kretzschmar HA (1994) Mouse cortical-cells lacking cellular PrP survive in culture with a neurotoxic PrP fragment. Neuroreport 5: 2057
110. Forloni G, Angeretti N, Chiesa R, Monzani E, Salmona M, Bugiani O, Tagliavini F (1993) Neurotoxicity of a prion protein fragment. Nature 362: 543
111. Supattapone S, Bosque P, Muramoto T, Wille H, Aagaard C, Peretz D, Nguyen HOB, Heinrich C, Torchia M, Safar J, Cohen FE, DeArmond SJ, Prusiner SB, Scott M (1999) Prion protein of 106 residues creates an artificial transmission barrier for prion replication in transgenic mice. Cell 96: 869
112. Khalili-Shirazi A, Kaisar M, Mallinson G, Jones S, Bhelt D, Fraser C, Clarke AR, Hawke SH, Jackson GS, Collinge J (2007) beta-PrP fom of human prion protein stimulates production of monoclonal antibodies to epitope 91-110 that recognise native PrPsc. Biochim Biophys Acta, Proteins Proteomics 1774: 1438
113. Peretz D, Williamson RA, Matsunaga Y, Serban H, Pinilla C, Bastidas RB, Rozenshteyn R, James TL, Houghten RA, Cohen FE, Prusiner SB, Burton DR (1997) A conformational transition at the N terminus of the prion protein features in formation of the scrapie isoform. J Mol Biol 273: 614
114. Yuan FF, Biffin S, Brazier MW, Suarez M, Cappai R, Hill AF, Collins SJ, Sullivan JS, Middleton D, Multhaup G, Geczy AF, Masters CL (2005) Detection of prion epitopes on PrPc and PrPsc of transmissible spongiform encephalopathies using specific monoclonal antibodies to PrP. Immunol Cell Biol 83: 632
115. Kaneko K, Ball HL, Wille H, Zhang H, Groth D, Torchia M, Tremblay P, Safar J, Prusiner SB, DeArmond SJ, Baldwin MA, Cohen FE (2000) A synthetic peptide initiates Gerstmann-Sträussler-Scheinker (GSS) disease in transgenic mice. J Mol Biol 295: 997
116. Kachel N, Kremer W, Zahn R, Kalbitzer HR (2006) Observation of intermediate states of the human prion protein by high pressure NMR spectroscopy. Bmc Structural Biology 6: 18
117. DeMarco ML, Daggett V (2004) From conversion to aggregation: Protofibril formation of the prion protein. Proc Natl Acad Sci USA 101: 2293
118. Supattapone S, Bouzamondo E, Ball HL, Wille H, Nguyen HOB, Cohen FE, DeArmond SJ, Prusiner SB, Scott M (2001) A protease-resistant 61-residue prion peptide causes neurodegeneration in transgenic mice. Mol Cell Biol 21: 2608
119. DeMarco ML, Silveira J, Caughey B, Daggett V (2006) Structural properties of prion protein protofibrils and fibrils: An experimental assessment of atomic models. Biochemistry 45: 15573
120. Govaerts C, Wille H, Prusiner SB, Cohen FE (2004) Evidence for assembly of prions with left-handed beta 3-helices into trimers. Proc Natl Acad Sci USA 101: 8342
121. Scouras AD, Daggett V (2008) Species variation in PrP^{Sc} protofibril models. J Mater Sci 43: 3625
122. Prusiner SB (1998) Prions. Proc Natl Acad Sci USA 95: 13363

123. Van der Kamp MW, Daggett V (2009) The consequences of pathogenic mutations to the human prion protein. Protein Engineering Design & Selection 22: 461
124. Chen W, Van der Kamp MW, Daggett V (2010) Diverse effects on the native β-sheet of the human prion protein due to disease-associated mutations. Biochemistry: In press
125. Rossetti G, Giachin G, Legname G, Carloni P (2010) Structural facets of disease-linked human prion protein mutants: A molecular dynamic study. Proteins: Struct Funct Bioinform DOI: 10.1002/prot.22834
126. Van der Kamp MW, Daggett V (2010) Pathogenic mutations in the hydrophobic core of the human prion protein can promote structural instability and misfolding. J Mol Biol DOI: 10.1016/j.jmb.2010.09.060
127. Zhang YB, Swietnicki W, Zagorski MG, Surewicz WK, Sonnichsen FD (2000) Solution structure of the E200K variant of human prion protein: Implications for the mechanism of pathogenesis in familial prion diseases. J Biol Chem 275: 33650
128. Rutherford K, Bennion BJ, Parson WW, Daggett V (2006) The 108M polymorph of human catechol O-methyltransferase is prone to deformation at physiological temperatures. Biochemistry 45: 2178
129. Rutherford K, Daggett V (2009) A Hotspot of Inactivation: The A22S and V108M Polymorphisms Individually Destabilize the Active Site Structure of Catechol O-Methyltransferase. Biochemistry 48: 6450
130. Rutherford K, Le Trong I, Stenkamp RE, Person VW (2008) Crystal structures of human 108V and 108M catechol O-methyltransferase. J Mol Biol 380: 120
131. Mead S (2006) Prion disease genetics. Eur J Hum Genet 14: 273
132. Goldfarb LG, Petersen RB, Tabaton M, Brown P, Leblanc AC, Montagna P, Cortelli P, Julien J, Vital C, Pendelbury WW, Haltia M, Wills PR, Hauw JJ, Mckeever PE, Monari L, Schrank B, Swergold GD, Autiliogambetti L, Gajdusek DC, Lugaresi E, Gambetti P (1992) Fatal Familial Insomnia and familial Creutzfeldt-Jakob disease: Disease phenotype determined by a DNA polymorphism. Science 258: 806
133. Brown DR (2000) Altered toxicity of the prion protein peptide PrP106-126 carrying the Ala(117) -> Val mutation. Biochem J 346: 785
134. McLean CA, Storey E, Gardner RJM, Tannenberg AEG, Cervenakova L, Brown P (1997) The D178N (cis-129M) "fatal familial insomnia" mutation associated with diverse clinicopathologic phenotypes in an Australian kindred. Neurology 49: 552
135. Swietnicki W, Petersen RB, Gambetti P, Surewicz WK (1998) Familial mutations and the thermodynamic stability of the recombinant human prion protein. J Biol Chem 273: 31048
136. Liemann S, Glockshuber R (1999) Influence of amino acid substitutions related to inherited human prion diseases on the thermodynamic stability of the cellular prion protein. Biochemistry 38: 3258
137. Apetri AC, Vanik DL, Surewicz WK (2005) Polymorphism at residue 129 modulates the conformational conversion of the D178N variant of human prion protein 90-231. Biochemistry 44: 15880
138. Chen SG, Zou W, Parchi P, Gambetti P (2000) PrP^{Sc} typing by N-terminal sequencing and mass spectrometry. Arch Virol: 209
139. Watanabe Y, Hiraoka W, Shimoyama Y, Horiuchi M, Kuwabara M, Inanami O (2008) Instability of familial spongiform encephalopathy-related prion mutants. Biochem Biophys Res Commun 366: 244
140. Billeter M, Wüthrich K (2000) The prion protein globular domain and disease-related mutants studied by molecular dynamics simulations. Arch Virol: 251

141. Gsponer J, Ferrara P, Caflisch A (2001) Flexibility of the murine prion protein and its Asp178Asn mutant investigated by molecular dynamics simulations. J Mol Graph Model 20: 169
142. Levy Y, Becker OM (2002) Conformational polymorphism of wild-type and mutant prion proteins: Energy landscape analysis. Proteins: Struct Funct Genet 47: 458
143. Shamsir MS, Dalby AR (2005) One gene, two diseases and three conformations: Molecular dynamics simulations of mutants of human prion protein at room temperature and elevated temperatures. Proteins: Struct Funct Bioinform 59: 275
144. Barducci A, Chelli R, Procacci P, Schettino V (2005) Misfolding pathways of the prion protein probed by molecular dynamics simulations. Biophys J 88: 1334
145. Riek R, Wider G, Billeter M, Hornemann S, Glockshuber R, Wüthrich K (1998) Prion protein NMR structure and familial human spongiform encephalopathies. Proc Natl Acad Sci USA 95: 11667
146. Hsiao K, Dlouhy SR, Farlow MR, Cass C, Dacosta M, Conneally PM, Hodes ME, Ghetti B, Prusiner SB (1992) Mutant prion proteins in Gerstmann-Straüssler-Scheinker disease with neurofibrillary tangles. Nat Genet 1: 68
147. Kitamoto T, Ohta M, Dohura K, Hitoshi S, Terao Y, Tateishi J (1993) Novel missense variants of prion protein in Creutzfeldt-Jakob disease or Gerstmann-Straüssler syndrome. Biochem Biophys Res Commun 191: 709
148. Peoc'h K, Manivet P, Beaudry P, Attane F, Besson G, Hannequin D, Delasnerie-Lauprêtre N, Laplanche J-L (2000) Identification of three novel mutations (E196K, V203I, E211Q) in the prion protein gene *PRNP* in inherited prion diseases with Creutzfeldt-Jakob disease phenotype. Hum Mutat 15: 482
149. Ripoll L, Laplanche JL, Salzmann M, Jouvet A, Planques B, Dussaucy M, Chatelain J, Beaudry P, Launay JM (1993) A new point mutation in the prion protein gene at codon 210 in Creutzfeldt-Jakob disease. Neurology 43: 1934
150. Nitrini R, Rosemberg S, PassosBueno MR, daSilva LST, Iughetti P, Papadopoulos M, Carrilho PM, Caramelli P, Albrecht S, Zatz M, LeBlanc A (1997) Familial spongiform encephalopathy associated with a novel prion protein gene mutation. Ann Neurol 42: 138
151. Apetri AC, Surewicz K, Surewicz WK (2004) The effect of disease-associated mutations on the folding pathway of human prion protein. J Biol Chem 279: 18008
152. Mishra RS, Bose S, Gu Y, Li R, Singh N (2003) Aggresome formation by mutant prion proteins: The unfolding role of proteasomes in familial prion disorders. J Alzheimer's Dis 5: 15
153. Silvestrini MC, Cardone F, Maras B, Pucci P, Barra D, Brunori M, Pocchiari M (1997) Identification of the prion protein allotypes which accumulate in the brain of sporadic and familial Creutzfeldt-Jakob disease patients. Nat Med 3: 521
154. Chebaro Y, Derreumaux P (2009) The conversion of helix H2 to beta-sheet is accelerated in the monomer and dimer of the prion protein upon T183A mutation. Journal of Physical Chemistry B 113: 6942
155. Kiachopoulos S, Bracher A, Winklhofer KF, Tatzelt J (2005) Pathogenic mutations located in the hydrophobic core of the prion protein interfere with folding and attachment of the glycosylphosphatidylinositol anchor. J Biol Chem 280: 9320
156. Zaidi SIA, Richardson SL, Capellari S, Song L, Smith MA, Ghetti B, Sy MS, Gambetti P, Petersen RB (2005) Characterization of the F198S prion protein mutation: Enhanced glycosylation and defective refolding. J Alzheimer's Dis 7: 159
157. Kovacs GG, Trabattoni G, Hainfellner JA, Ironside JW, Knight RSG, Budka H (2002) Mutations of the prion protein gene: Phenotypic spectrum. J Neurol 249: 1567
158. Piccardo P, Liepnieks JJ, William A, Dlouhy SR, Farlow MR, Young K, Nochlin D, Bird TD, Nixon RR, Ball MJ, DeCarli C, Bugiani O, Tagliavini F, Benson MD,

Ghetti B (2001) Prion proteins with different conformations accumulate in Gerstmann-Sträussler-Scheinker disease caused by A117V and F198S mutations. Am J Pathol 158: 2201

159. Caughey B, Race RE, Ernst D, Buchmeier MJ, Chesebro B (1989) Prion protein biosynthesis in scrapie-infected and uninfected neuroblastoma cells. J Virol 63: 175
160. Endo T, Groth D, Prusiner SB, Kobata A (1989) Diversity of oligosaccharide structures linked to asparagines of the scrapie prion protein. Biochemistry 28: 8380
161. Hornemann S, Schorn C, Wüthrich K (2004) NMR structure of the bovine prion protein isolated from healthy calf brains. Embo Reports 5: 1159
162. Stadtman ER, Van Remmen H, Richardson A, Wehr NB, Levine RL (2005) Methionine oxidation and aging. Biochim Biophys Acta, Proteins Proteomics 1703: 135
163. Canello T, Engelstein R, Moshel O, Xanthopoulos K, Juanes ME, Langeveld J, Sklaviadis T, Gasset M, Gabizon R (2008) Methionine sulfoxides on PrP^{Sc}: A prion-specific covalent signature. Biochemistry 47: 8866
164. Silva CJ, Onisko BC, Dynin I, Erickson ML, Vensel WH, Requena JR, Antaki EM, Carter JM (2010) Assessing the role of oxidized methionine at position 213 in the formation of prions in hamsters. Biochemistry 49: 1854
165. Wolschner C, Giese A, Kretzschmar HA, Huber R, Moroder L, Budisa N (2009) Design of anti- and pro-aggregation variants to assess the effects of methionine oxidation in human prion protein. Proc Natl Acad Sci USA 106: 7756
166. Lisa S, Meli M, Cabello G, Gabizon R, Colombo G, Gasset M (2010) The structural intolerance of the PrP α-fold for polar substitution of the helix-3 methionines Cell Mol Life Sci: 10.1007/s00018
167. Tatzelt J, Prusiner SB, Welch WJ (1996) Chemical chaperones interfere with the formation of scrapie prion protein. EMBO J 15: 6363
168. Bennion BJ, DeMarco ML, Daggett V (2004) Preventing misfolding of the prion protein by trimethylamine N-oxide. Biochemistry 43: 12955
169. Granata V, Palladino P, Tizzano B, Negro A, Berisio R, Zagari A (2006) The effect of the osmolyte trimethylamine N-oxide on the stability of the prion protein at low pH. Biopolymers 82: 234
170. Wang A, Bolen DW (1997) A naturally occurring protective system in urea-rich cells: Mechanism of osmolyte protection of proteins against urea denaturation Biochemistry 36: 9101
171. Bennion BJ, Daggett V (2004) Counteraction of urea-induced protein denaturation by trimethylamine N-oxide: A chemical chaperone at atomic resolution. Proc Natl Acad Sci USA 101: 6433
172. Zou Q, Bennion BJ, Daggett V, Murphy KP (2002) The molecular mechanism of stabilization of proteins by TMAO and its ability to counteract the effects of urea. J Am Chem Soc 124: 1192
173. Kuwata K, Nishida N, Matsumoto T, Kamatari YO, Hosokawa-Muto J, Kodama K, Nakamura HK, Kimura K, Kawasaki M, Takakura Y, Shirabe S, Takata J, Kataoka Y, Katamine S (2007) Hot spots in prion protein for pathogenic conversion. Proc Natl Acad Sci USA 104: 11921
174. Yamamoto N, Kuwata K (2009) Regulating the conformation of prion protein through ligand binding. Journal of Physical Chemistry B 113: 12853

Fig. 1. Structure of the human prion protein. (a) The mature human prion protein as it can be found on the outer cell membrane. The GPI-anchor (attached to Ser230) and typical glycans (attached to Asn181 and Asn197) are shown in sticks. Structure obtained from MD simulation (Van der Kamp, Koldsø and Daggett, unpublished results). (b) The structured part of the recombinant human prion protein, as obtained by protein NMR [39]. Secondary structure elements are labeled.

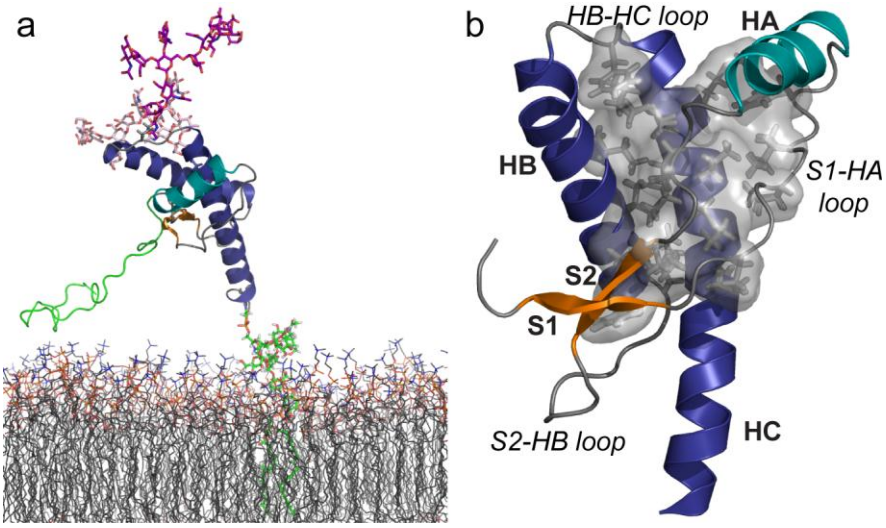

Fig. 2. Conformational changes in the globular domain of PrP induced by acidic pH [59]. (a) Snapshots from a simulation at acidic pH, indicating the loss of hydrophobic contacts between the S1-HA loop and HC, followed by displacement of the N-terminal end of HA. (b) Cα traces of simulations at neutral, mildly acidic and strongly acidic pH from left to right. Structures of 5 simulations at each pH regime are shown for every 1 ns in the 25-50 ns time interval. The parts of HB and HC that remain stable (in agreement with experiment) are indicated by darker colors. In both panels, N-terminal residues 90-124 are omitted for clarity.

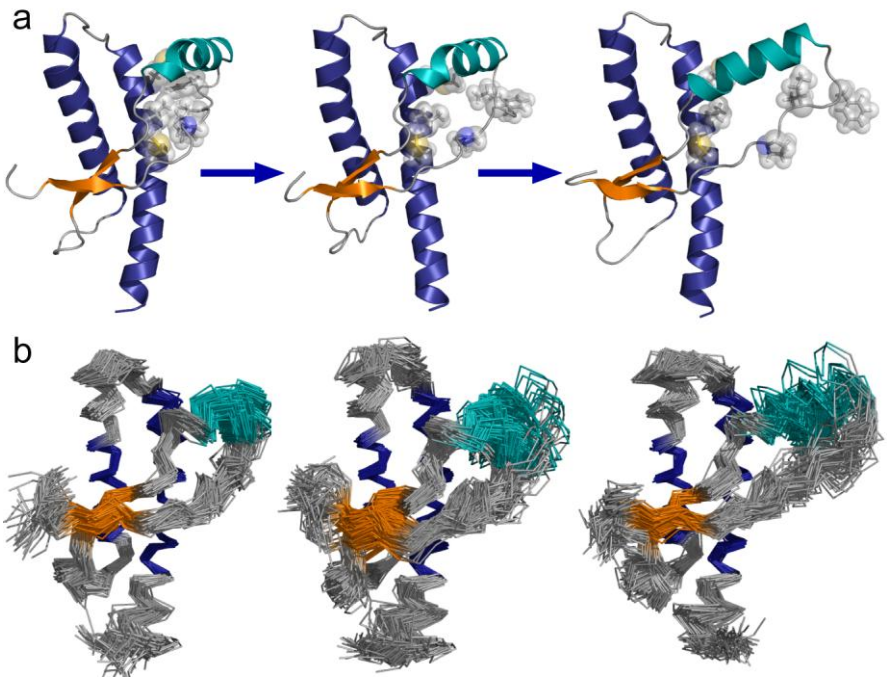

Fig. 3. Potential misfolding and aggregation of PrP. (a) Misfolding of D147N hamster PrP observed in simulation at strongly acidic pH and docking of three misfolded monomers into an intial aggregate [117]. (b) Spiral protofibril models (built up from 6 monomers each) for D147N hamster PrP (as shown in panel a), bovine PrP and human PrP [121].

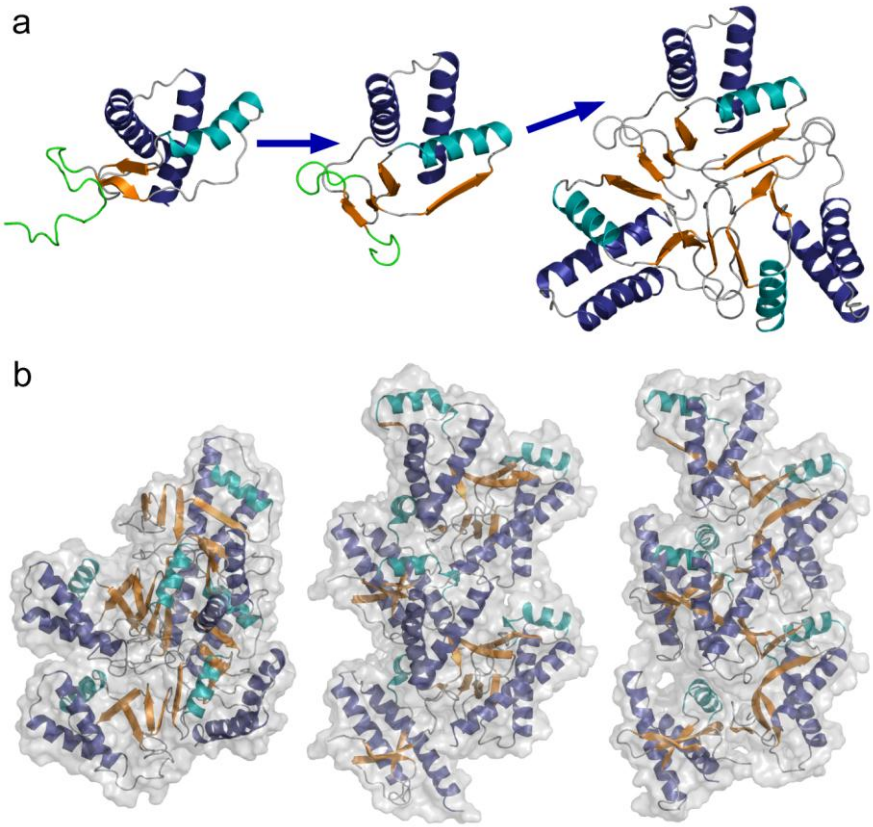

Fig. 4. Changes in conformation and flexibility caused by pathogenic mutations [126]. (a) Typical conformation and flexibility for WT PrP, T183A PrP and F198S PrP. Only the globular domain (res. 128-228) is shown. Flexibility is indicated by the thickness of the ribbon and the mutation site is indicated by a red sphere. (b) Early misfolding events in a simulation of V180I PrP. First, an additional strand appears on the native sheet. Thereafter, hydrophobic contacts between HC and the S1-HA loop are lost and HA moves out to solvent. Mutation site is indicated by a sphere. For clarity, res. 90-112 are omitted.

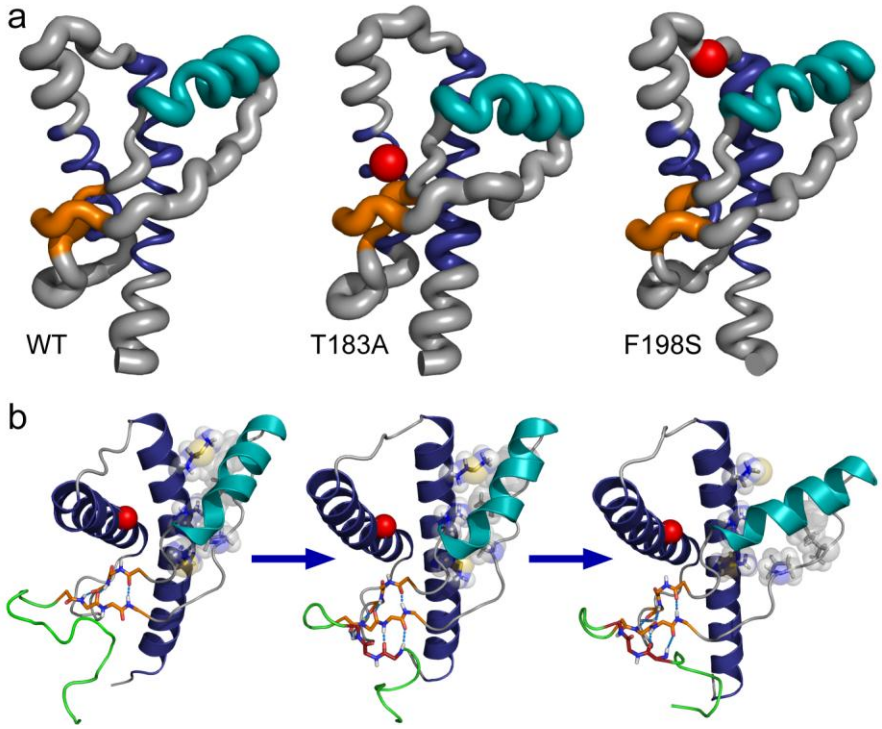

Fig. 5. The effect of TMAO on PrP structure and misfolding. Starting from natively folded hamster recPrP (res. 109-219), simulation at acidic pH in water causes conversion to a misfolded form [56]. In the presence of 1M TMAO, however, the structure is protected from misfolding (protection) and the extended sheet in the misfolded conformation dissolves (reversion) [168]. An Ω-loop conformation (green) in the flexible N-terminus is observed in the presence of TMAO.

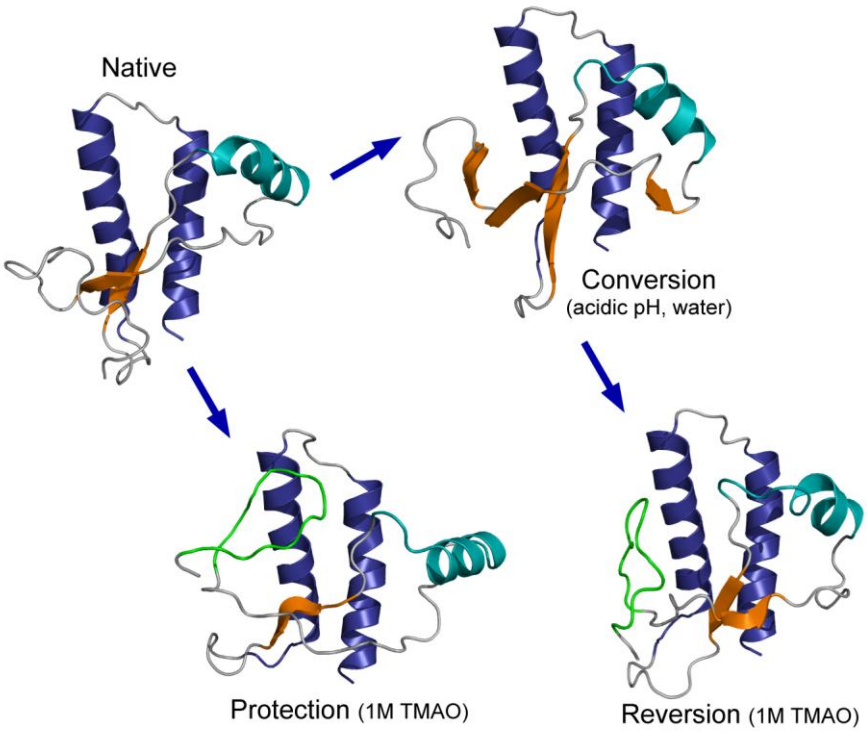

Graphical abstract